

Mechanism of charge transport in discotic liquid crystals

N. Boden, R. J. Bushby, J. Clements, and B. Movaghar

Centre for Self-Organising Molecular Systems and the School of Chemistry, The University of Leeds, Leeds LS2 9JT, United Kingdom

K. J. Donovan and T. Kreouzis

Department of Physics, Queen Mary and Westfield College, London, E1 4NS United Kingdom

(Received 21 February 1995)

A comparative study is reported of transient photoconductivity and ac conductivity in the liquid-crystalline columnar hexagonal (D_h) phase of pure and p -doped hexakis(n -hexyloxy)triphenylene. In both materials, charge-carrier transport is dispersive, and the measured carrier mobilities along the direction of the molecular columns are very similar, $\mu_{\parallel} \sim 1 \times 10^{-4} \text{ cm}^2 \text{ V}^{-1} \text{ s}^{-1}$. The dispersion arises from the intrinsic liquidlike disorder in the face-to-face packing of the triphenylene rings within the columns. Charge transport is found to be highly anisotropic ($\mu_{\parallel}/\mu_{\perp} \sim 10^3$). These results are discussed in terms of possible mechanisms for carrier transport in discotic liquid crystals.

I. INTRODUCTION

Discotic liquid crystals are comprised of disordered stacks (one-dimensional fluids) of disc-shaped molecules arranged on a two-dimensional lattice.¹ This structure imparts properties on these materials from which applications are likely to stem. One such property is the transport of charge along the molecular stacks.²⁻⁷ The separation between the aromatic cores in, for example, the hexakis(n -alkoxy)triphenylene (HATn), the archetypal discotic liquid crystal, Fig. 1, is of the order of 3.5 Å, so that considerable overlap of π^* orbitals of adjacent aromatic rings is expected to lead to quasi-one-dimensional conductivity. However, the hexakis(n -alkoxy)triphenylene (HATn) have a very low intrinsic carrier concentration, due in part to the fairly large band gap in these materials ($\sim 4 \text{ eV}$),⁸ and are therefore insulators. Nevertheless, the low oxidation potential of the hexakis(n -alkoxy)triphenylene (HATn) facilitates the formation of radical cations upon the introduction of electron acceptors into the insulating hydrocarbon matrix surrounding the aromatic cores, making these materials good conductors.^{2,3}

For example, when an electron acceptor such as AlCl_3 or NOBF_4 is dissolved into the hydrocarbon chain matrix, an electron is extracted from the triphenylene core leading to the formation of a radical cation.⁹ It has been established that the presence of these radical cations gives rise to charge-carrier migration along the columns of triphenylene cores.³ The level of conductivity of these quasi-one-dimensional

semiconductors can be varied by varying the degree of charge transfer (0–0.15), which is governed by the stoichiometry.

Of particular interest, it has been shown that charge transport along the direction of the columns in these doped materials is dispersive,³ and also that the conductivity σ_{\parallel} varies linearly with the concentration of dopant. We may therefore conclude from $\sigma_{\parallel} = ne\mu_{\parallel}$, where n is the density of carriers and e is the electronic charge, that μ_{\parallel} is a constant ($\mu_{\parallel} \sim 1 \times 10^{-4} \text{ cm}^2 \text{ V}^{-1} \text{ s}^{-1}$ at 350 K). It appears that the mobility of the charge carriers is not detectably influenced by the nature or concentration of the dopant counterions (AlCl_4^- , BF_4^-) at prevailing temperatures. However, recent measurements of transient photoconductivity in the D_h phase of hexakis(n -pentyloxy)triphenylene (HAT5) (Refs. 10 and 11) have indicated an intrinsic, bandlike transport mechanism, despite the value of the mobility ($\mu_{\parallel} \sim 1 \times 10^{-3} \text{ cm}^2 \text{ V}^{-1} \text{ s}^{-1}$ at 350 K) appearing to be too low. For bandlike transport in molecular crystals one would expect $\mu_{\parallel} \geq 1 \text{ cm}^2 \text{ V}^{-1} \text{ s}^{-1}$. These observations raise the interesting question as to whether in the chemically doped material the dispersive transport owes its origin to the presence of the counterions, or to the intrinsic disorder in the molecular packing in the columnar stacks. If it were to be the latter, dispersive transport would be expected to occur in the transient photoconductivity experiments as well. To resolve this issue, we have carried out comparative studies of the ac conductivity of hexakis(n -hexyloxy)triphenylene (HAT6) doped with NOBF_4 and the transient photoconductivity of the undoped material. It will be shown that charge transport is intrinsically dispersive in both these materials.

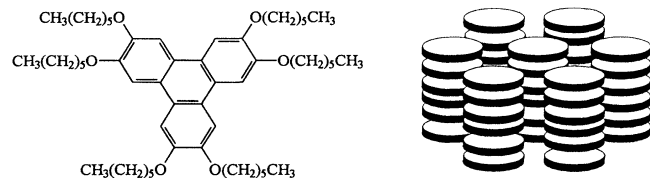


FIG. 1. Hexakis(n -hexyloxy)triphenylene (HAT6) and a schematic view of its columnar D_h mesophase.

II. EXPERIMENTS AND RESULTS

HAT6 was synthesized as described previously.¹² It was purified by flash chromatography followed by several crystallizations. The resulting material displayed a hexagonal columnar D_h mesophase in the temperature range 343 to 374 K

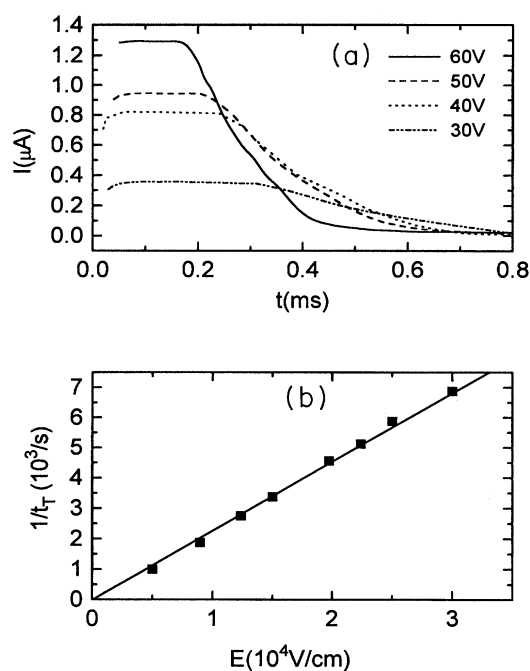


FIG. 2. (a) Transient photoconductivity hole transients in the D_h phase of HAT6 at 359 K. (b) The variation of reciprocal transit time for holes, in the D_h phase of HAT6 at 359 K, with applied electric field.

(Ref. 3) as measured by differential scanning calorimetry, compared with literature values of 341 to 372 K.¹³

For the transient photoconductivity measurements, HAT6 was held between two quartz slides which had semitransparent aluminum electrodes evaporated upon them. Thin samples of HAT6 are easily aligned homeotropically by slow cooling from the isotropic phase into the mesophase, yielding relatively large uniform domains. The slides were separated by 20 μm thick Mylar spacers and held in the D_h phase at 359 K in a temperature controlled block. A voltage V was applied to the top electrode whilst the bottom controlled block. A voltage V was applied to the top electrode whilst the bottom electrode was connected via a preamplifier with a 1 $\text{k}\Omega$ input resistance to an oscilloscope. Photocarriers were excited within a skin depth $d < 1 \mu\text{m}$ of the top electrode with a nitrogen laser of pulse width 6 ns, $\hbar\omega = 3.68 \text{ eV}$ ($\lambda = 337 \text{ nm}$). Laser irradiation into the main absorption band of HAT6 leads to the creation of electron-hole pairs. Depending upon the polarity of the external field, electrons or holes drift across the sample cell producing a displacement current $I(t)$, which was recorded in the external circuit. When the top electrode was negative (electron drift) rapidly decaying currents were observed. We interpret this as due to electrons being trapped in a very short distance from the top electrode by residual oxygen at the surface. In contrast, when the top electrode was positive (hole drift), well defined current transients were observed, Fig. 2(a). It is seen that a plateau region is followed at the transit time t_T by a transition to a long-time tail. t_T is related to the average drift velocity $v = l/t_T$ which, in turn, is linearly related to the elec-

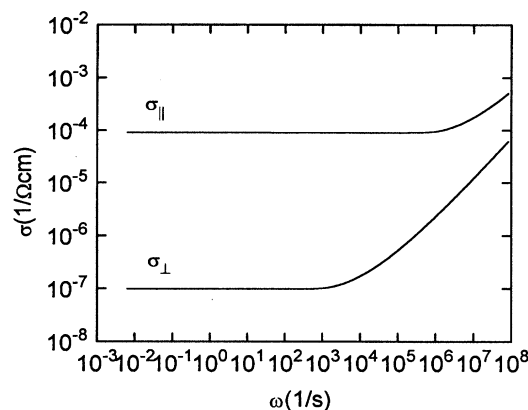


FIG. 3. Alternating current conductivities parallel σ_{\parallel} and perpendicular σ_{\perp} to the axes of the columns of HAT6/NOBF₄ ($x=0.01$) in the D_h phase at 350 K.

tric field E via the mobility μ , $v = \mu E$, provided Ohm's law holds. The effective carrier mobility μ is therefore given by

$$\mu = l^2/t_T V, \quad (1)$$

where l is the sample thickness. From the slope of the line in Fig. 2(b), a hole mobility of $\mu_{\parallel} = (4.4 \pm 0.05) \times 10^{-4} \text{ cm}^2 \text{ V}^{-1} \text{ s}^{-1}$ is obtained at 359 K.

Doped samples for impedance spectroscopy studies were prepared by making up dilute solutions of HAT6 (predegassed by means of several melt-pump-freeze cycles) and NOBF₄ in dichloromethane, of appropriate concentration. These were mixed in a large glass vessel, which was then attached to a high vacuum line to remove the solvent. The vessel was opened in an anaerobic glovebox ($\text{O}_2 < 5 \text{ ppm}$, $\text{H}_2\text{O} < 10 \text{ ppm}$) and the doped HAT6 transferred into the measurement cell. Alternating current (1 mHz–13 MHz) electrical conductivity measurements were made using both a Schlumberger-Solartron 1253 gain-phase analyzer (1 mHz–20 Hz) and a Hewlett-Packard 4192A Impedance Analyzer (5 Hz–13 MHz) with a cell employing a four-terminal pair electrode configuration on samples 200 μm thick. Sample temperature was controlled to within 100 mK using a N_2 gas-flow system and an Oxford Instruments DTC 2 temperature controller. The samples were aligned by slowly cooling from the isotropic phase into the columnar phase in the presence of a magnetic field, $B = 2.2 \text{ T}$.^{3,14}

Typical measurements of the frequency dependence of the conductivity are shown in Fig. 3. For both σ_{\parallel} and σ_{\perp} a $\omega^{0.8}$ frequency dependence is found at higher frequencies. At lower frequencies, σ is independent of frequency. The low-frequency value of σ_{\parallel} is approximately 10^3 times the corresponding value of σ_{\perp} . This shows that the conductivity is highly anisotropic. The variation of both σ_{\parallel} and σ_{\perp} with frequency is characteristic of dispersive transport.¹⁵ It is typically observed where charge carriers hop from site-to-site with a distribution of hopping probabilities.

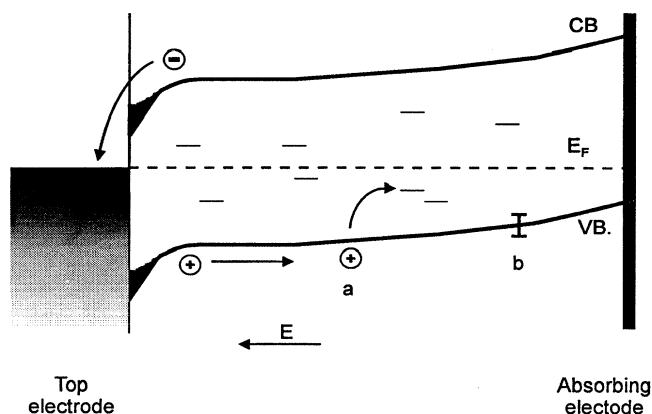


FIG. 4. Schematic band diagram for a narrow-band photoconductor showing the trapping of a hole into an occupied state below the Fermi energy, E_F (a) and the amplitude of typical fluctuations in the bandwidth due to the liquidlike fluctuations in the columnar order (b).

III. DISCUSSION

Comparison of transport in pure and doped HAT6

In Fig. 4 we show a schematic band diagram for a narrow-band photoconductor such as pure HAT6. The appearance of the photocurrent transients shown in Fig. 2 can be easily rationalized in terms of this simple band structure. The plateau region corresponds to the hole space charge sheet drifting to the absorbing electrode through the valence band. The liquidlike, self-organizing nature of the molecular columns causes bandwidth fluctuations, and rapidly anneals away the majority of defects in columnar organization. Thus the majority of carriers drift across the sample without significant trapping. However a minority of carriers are trapped at impurity sites (occupied states in the band gap below the Fermi level) and give rise to the long-time tail observed in the photocurrent transients. It is well known that in time-of-flight measurements, the presence of impurities can have a significant effect on the observed photocurrent transients.¹⁶ Although there is undoubtedly some degree of impurity trapping in these discotic liquid crystals, we believe that the intrinsic liquidlike disorder in the columns combined with the dynamical fluctuations in the molecular positions present at ambient temperatures determines the transport mechanism.

Figure 5(a) shows a schematic band structure for doped HAT6. The dopant removes electrons leaving columnar electronic diffusive levels at the top of the valence band. Thus we envisage that the charge carriers migrate along the columns hopping from one molecular to the next within this energy band, subject to fluctuations in intermolecular separation and/or the effects of defects in the columnar organization, as shown schematically in Fig. 5(b). As a result, the charge carriers experience a fluctuating potential $V(r)$ as shown in Fig. 5(c).

The frequency dependence of σ_{\parallel} observed is of the form

$$\sigma(\omega) = \sigma(0) + A\omega^s, \quad (2)$$

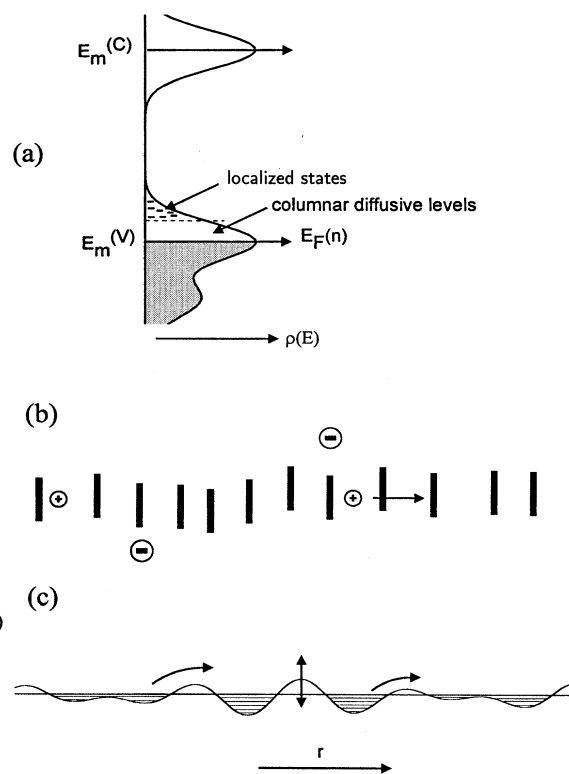


FIG. 5. (a) Schematic diagram showing the density of states for doped HAT6. $E_m(C)$ and $E_m(V)$ represent the conduction and valence molecular energy bands, respectively, and $E_F(n)$ is the Fermi energy which is dependent on the number of carriers. (b) Schematic representation of a molecular column showing the diffusing charge carriers, the counterions and the fluctuations in the columnar order. (c) Schematic diagram representing the potential $V(r)$ seen by charge carrier diffusing along the molecular column. The vertical arrow represents the fluctuation in this potential due to the liquidlike fluctuations in the columnar order.

where $s \sim 0.8$. This type of behavior is characteristically observed in a whole range of disordered materials.¹⁷ One cause of such behavior is where charge carriers hop from site to site with a distribution of hopping probabilities. In the case of HAT6, we believe that such a distribution arises from the liquidlike disorder of the molecular packing in the columns [see Fig. 5(b)]. At high frequencies, the charge carriers are presumably hopping between neighboring aromatic cores with a broad distribution of transition rates, whilst the frequency independence of σ seen at low frequencies is associated with the slowest transition rate. We believe this to be associated with either the largest intermolecular separation within the columns or with structural defects and impurities. This type of behavior can be modeled using the theory of Alexander *et al.*¹⁸ for charge carriers hopping from one site to the next in one dimension with a distribution of hopping probabilities.

At low frequencies, an estimate of the charge-carrier mobility along the columns μ_{\parallel} can be made using $\sigma_{\parallel}(0) = ne\mu_{\parallel}$. This requires a value for the density of charge

carriers n . We have estimated a value of $n = 1.08 \times 10^{19} \text{ cm}^{-3}$ from spin susceptibilities measured by electron-spin resonance² using DPPH as a calibration standard: that is, we have assumed the absence of deep trapping of charge carriers, and that there are no spinless charge carriers. A charge-carrier mobility $\mu_{\parallel} = (8.5 \pm 0.4) \times 10^{-5} \text{ cm}^2 \text{ V}^{-1} \text{ s}^{-1}$ at 350 K has been calculated on this basis. Thus, we have the surprising result that the charge-carrier mobility estimated from the conductivity of doped HAT6 and that measured in the time-of-flight experiment on pure HAT6, $\mu_{\parallel} = (4.4 \pm 0.05) \times 10^{-4} \text{ cm}^2 \text{ V}^{-1} \text{ s}^{-1}$, are very similar. The dopant appears to generate charge carriers without introducing a significant concentration of charge-carrier traps.

At first sight, this appears to be paradoxical, since the Coulombic field of the counterions is expected to be efficient at trapping charge carriers. However, at ambient temperatures, the dynamical fluctuations in the positions of the molecules within the columns will give rise to phonon-assisted tunneling processes within the discotic band. In addition, the tunneling barrier caused by the nearest counterion is itself modulated by the dynamics of *all the other* charges in the system. When the charge-carrier diffusion coefficient parallel to the column axes D_{\parallel} is finite, the influence of the Coulombic fields is averaged out on the time scale $l_d^2/4D_{\parallel}$ where l_d is the average separation between dopant counterions. At low enough temperatures, the thermal fluctuations will be frozen out leaving only quantum fluctuations. If the total bandwidth is then small compared to the effective trapping potential, we will obtain an insulator. In “insulators,” charge-carrier diffusivity is a strong function of temperature. At the moment, we do not know whether doped samples exhibit hopping or trap-limited transport behavior. If the apparent activation energy $E_a \sim 0.5 \text{ eV}$ observed³ is genuinely associated with a trapping process, and not simply a result of thermally assisted transport in an already “conducting medium,” then the mobility should be written as

$$\mu(T) = \mu_0 e^{-E_a/kT}, \quad (3)$$

with $E_a \sim 0.5 \text{ eV}$. This gives an intrinsic column mobility of $\mu_0 \sim 10^3 \text{ cm}^2 \text{ V}^{-1} \text{ s}^{-1}$, a high value even for the purest molecular crystals. Time-of-flight measurements on discotic liquid crystals give mobilities of at most $\mu_0 \sim 10^{-1} \text{ cm}^2 \text{ V}^{-1} \text{ s}^{-1}$, at the lowest temperature measured, $T \sim 300 \text{ K}$.¹⁹ This is reasonable for a “stochastic” mobility as it gives a jump rate of the order $W_{\parallel} \sim 10^{12} \text{ s}^{-1}$ from molecule to molecule. Quantum-mechanical band mobilities in discotic liquid crystals at very low temperatures, and in the absence of disorder may perhaps reach values of up to $10 \text{ cm}^2 \text{ V}^{-1} \text{ s}^{-1}$. So we conclude that the temperature dependence of the type in Eq. (3) is probably not the correct way of expressing μ as a function of temperature. We expect μ to be a weaker function of T , and specially for highly doped samples. Modeling of doped polymers^{20,21} suggests behavior of the form

$$\mu(T) = \mu_0 e^{-[T_0/T_1 + T]^{\xi}} \quad (4)$$

with $0 < \xi < 1$. The parameters T_0 and T_1 are measures of typical tunneling barrier height and inverse width, respec-

tively. The latter, namely $T_1(n)$, is a function of dopant density n such that $T_1 \rightarrow 0$ as $n \rightarrow n_c$, where n_c is the critical density for localization.

We have seen that a model based on hopping between aromatic cores of neighboring molecules, subject to fluctuations in intermolecular separation and/or the effects of defects in the columnar organization, can account for many of the features of the conductivity behavior of doped HAT6 in the vicinity of room temperature. In the time-of-flight experiment, the current transients shown in Fig. 2(a) are typical of a system characterized by multiple shallow trapping, where charge carriers are subject to a sequence of trapping and release events, with only a fraction of the charge carriers being momentarily free to move.¹⁶ Thus, it seems that the triphenylene cores in the molecular stacks act as shallow trapping sites. We believe that it must be for the following reason. At high temperatures in the ordered liquid crystalline phase, “disorder” is dynamic and self-repairing²² on the time scale of the electronic diffusion process. However, there are also excitation processes giving rise to disorder which are slow on this timescale. For example, a HAT6 molecule can move laterally out of its columnar position,²³ and stay there longer than a time of order 10^{-12} s and cause a major obstacle or trap to a carrier moving along the columns. At low temperatures, we expect there to be “frozen-in” disorder which would manifest itself in a temperature-dependent mobility of the type shown in Eq. (4) with $\xi \sim 2$. Indeed, this is a common observation in nonequilibrium transport in pure molecular crystals.²⁴ Thus measurements at lower temperatures than have been studied to date are imperative.

Charge transport in pure HAT6

Despite the well-defined transits shown in Fig. 2, the absolute mobilities are lower than for molecular crystals. This is presumably due to the high anisotropy of these systems, amplifying the effect of static and dynamic fluctuations for transport along one-dimensional columns.

Combining the data in Ref. 3 with time-of-flight data^{10,11,18} and that of the present paper, the following transport picture emerges. Charge transport in aligned discotics is highly one dimensional. Dispersion in the crystalline phase is due to misalignment of columns, and dislocations. These structural defects give rise to shallow and deep traps which will largely disappear as soon as the system enters the liquid crystalline phase.²² The structural traps are removed by the columnar fluctuations allowing the charge carriers to move along the columns subject only to time-dependent potentials resulting from molecular motions. The amplitude of these potential fluctuations are small compared to the bandwidth, which is of order 0.2 to 0.4 eV.⁸

The time-of-flight mobility $\mu_{\parallel}(T)$ in hexahexylthiotriphenylene¹⁷ exhibits discontinuities in going from the one phase to another: These range from $\mu_{\parallel} = 10^{-1} \text{ cm}^2 \text{ V}^{-1} \text{ s}^{-1}$ in the helical discotic phase to $\mu_{\parallel} = 10^{-3} \text{ cm}^2 \text{ V}^{-1} \text{ s}^{-1}$ in the D_h phase to $\mu_{\parallel} = 10^{-4} \text{ cm}^2 \text{ V}^{-1} \text{ s}^{-1}$ in the isotropic phase. The decrease in this one-carrier mobility is presumably caused by dynamical fluctuations. In doped HAT6, as already discussed, we observe a gradual increase of both σ_{\parallel} and σ_{\perp} with temperature.³ The change is less than an order of magnitude (~ 5) in the temperature range 300 to

350 K. [At low temperatures we expect behavior of the type shown in Eq. (4) with $\zeta=2$ and $T_1=0$ (Ref. 24).] This increase is probably due to thermally assisted detrapping of charge carriers. We shall see that in doped HAT6, the motion of a carrier along a column is severely limited by the dynamics of its neighbors. A trapped carrier will provide a barrier hindering the migration of other carriers along the same column. Transverse excitation of such trapped carriers will therefore have an important role in determining the carrier mobility μ_{\parallel} .

Charge transport in doped HAT6 along the columns

The exponent of the $\omega^{0.8}$ law for the ac conductivity remains essentially identical for $\sigma_{\parallel}(\omega)$ when going from the solid ($T=300$ K) to the liquid crystalline phase ($T=350$ K), whereas s changes from ~ 0.75 to ~ 0.8 for $\sigma_{\perp}(\omega)$.³ This implies that $\sigma_{\perp}(\omega)$ saturates (i.e., becomes independent of ω at high frequencies) at a larger value in the D_h phase. In the 10 GHz regime, the difference between solid and liquid crystalline values of $\sigma_{\perp}(\omega)$ could well be one or two orders of magnitude and this would indeed be in line with observations made on a phthalocyanine-based discotic by time-resolved microwave conductivity.²⁵

In the temperature range of current interest, 300–400 K, the conductivity rises linearly with doping concentration³ indicating that the charge carriers are relatively free to move along the stacks (μ is only weakly temperature and field dependent). With dopant concentrations of the order of 1×10^{19} cm³, the distance between neighboring charge carriers in the columns is, on average, 300 Å, which gives rise to a considerable Coulomb field ($e^2/4\pi\epsilon\epsilon_0 \geq 0.05$ eV). This implies that electronic correlations play a significant role in determining the low-temperature band structure and transport mechanism.

Analyzing the conductivity of the system from the point of view of an anisotropic resistor network, however, allows us to avoid the subtle many-body phenomena implicit in this problem. The length scale of the resistance is the average distance between the dopant counterions l_d . Beyond this length scale, carriers see roughly the “same world” again. The fluctuations can thus be represented by a distribution of resistances. Individual charge dynamics in the present temperature range can be analyzed using one-body time-dependent rates and by treating the field due to the remaining charge carriers (and ions and molecular dipoles) as an effective fluctuating field. The charge carriers move in the presence of the total time-dependent fluctuating field $\mathcal{V}(\mathbf{r}, t)$ where

$$\mathcal{V}(\mathbf{r}, t) = \mathcal{V}_{\text{electrons or holes}}(\mathbf{r}, t) + \mathcal{V}_{\text{ions}}(\mathbf{r}, t) + \mathcal{V}_{\text{electron-phonons}}(\mathbf{r}, t). \quad (5)$$

To a first approximation, we can divide the dynamics into a fast component modulating the transition from one molecular to the next, and the slow component of the larger amplitude fluctuations which gives rise to a quasistatic potential disorder. In this picture, which eliminates the intermediate dynamics, the charge moves as a stochastic random walker with a distribution of jump rates $P[W_{\parallel}]$ and $P[W_{\perp}]$. In one di-

mension this problem can be solved exactly,²⁶ but in quasi-three-dimensions the bond coherent-potential approximation gives very good results.²⁷

The observed frequency-dependent conductivity of doped HAT6 confirms this type of stochastic approach. The onset of the frequency dependence is then related to time scales faster than the slowest transfer rates encountered. The situation of $\sigma(\omega)$ will occur when the fastest microscopic rates have been reached. Along the columns we can expect the fastest rates to be in the range 10^{10} – 10^{12} s⁻¹ and therefore far higher than the highest frequency measured (8×10^7 s⁻¹).

Charge transport in doped HAT6 perpendicular to the columns

The transport perpendicular to the columns in a more complex phenomenon. The charge has to cross an insulating hydrocarbon region of at least 15 Å. The transfer cannot be simple (elastic) quantum-mechanical tunneling. A simple estimate using an exponential wave-function overlap with $W_{\perp} \approx W_0 e^{-2\alpha\bar{R}}$ leads to a reduction of order 10^{-6} with respect to W_{\parallel} , with $\bar{R} \sim 15$ Å and $\alpha \sim 2$ Å. Intercolumnar transport at low temperatures can only take place at dislocations, or with the assistance of *defect bridges*. At high temperatures [300–400 K], the transfer process must be a complex many-phonon assisted (time-dependent) tunneling process. The total amplitude is therefore a sum over a large class of alternative dynamical pathways.^{28,29} The charge carrier will execute a complex random-walk process in time, scattering frequently from the insulating side chains, until finally, with the help of a *favorable strong fluctuation* it will cross between columns. In this sense, the process is comparable to a Marcus transition.³⁰ This process is also likely to be strongly assisted by the presence of a dynamical external field, such as an ac electric field. In contrast to ordinary stochastic hopping,¹⁷ where Fermi golden rule transfer rates (W_{\perp}) apply, the time dependence of $W_{\perp}(t)$, corresponding to the actual dynamical transfer process, will itself be affected by a high-frequency field. This implies that the hop rate W is a function of the ac frequency, i.e., $W(\omega)$. We must conclude therefore that the elementary rate cannot be computed by a simple Fermi golden rule approach, but should rather be treated as a fully time-dependent tunneling process assisted by many pathways. The high-frequency $\sigma_{\perp}(\omega)$ is thus a reflection of time-dependent tunneling dynamics rather than a golden rule rate with,

$$\sigma_{\parallel, \perp}(\omega) \sim \frac{e^2}{kT} \sum_{i,j,\sigma} \{R_{ij}^2 W_{ij}^{\perp, \sigma}(\omega)\} F_{i,\sigma} [1 - F_{j,\sigma}], \quad (6)$$

where $F_{i,\sigma}$ is the Fermi function at a molecular or transport site i , R_{ij} is a jump distance and $W_{ij}(\omega)$ is the frequency-dependent jump rate normally considered to be the first order (unrenormalized) golden rule transition rate given by

$$W_{ij} = \nu_0 e^{-2\alpha R_{ij}} e^{-[E_j - E_i]/kT}. \quad (7)$$

The anisotropy of the conductivity is of order

$$\lim_{\omega \rightarrow \infty} \left(\frac{\sigma_{\parallel}}{\sigma_{\perp}} \right) \sim \frac{\bar{a}_{\parallel}^2 \left[\frac{\bar{W}_{\parallel}}{\bar{W}_{\perp}} \right]}{\bar{a}_{\perp}^2 \left[\frac{\bar{W}_{\perp}}{\bar{W}_{\parallel}} \right]}, \quad (8)$$

where \bar{a}_{\parallel} and \bar{a}_{\perp} are average lattice parameters ($\bar{a}_{\parallel} \sim 3.5 \text{ \AA}$ and $\bar{a}_{\perp} \sim 19.5 \text{ \AA}$). This anisotropy is larger than the ratio that we can expect from Fig. 3. We conclude therefore, that $W_{\perp}(\omega)$ is frequency dependent, and has dynamically assisted "tunneling" contributions. Thus, we also expect $\{W_{\perp}(\omega)_{lc}/W_{\perp}(\omega)_c\}$, where $W_{\perp}(\omega)_{lc}$ and $W_{\perp}(\omega)_c$ are the frequency-dependent jump rates in the liquid crystalline and crystalline phases, respectively, to increase with ω and to be larger than the corresponding ratio in the present experimental range.

We should note that the intercolumnar transport can also be assisted or even dominated by ionic exchange processes. In the D_h mesophase the molecular diffusion coefficient perpendicular to the columns is of the order of $D_m \sim 5 \times 10^{-11} \text{ m}^2 \text{ s}^{-1}$.²³ If we assume that a charged molecule moves roughly in the same way as an uncharged molecule, then this ionic diffusivity exceeds the supposedly electronic one, $D_{\perp} \sim 5 \times 10^{-13} \text{ m}^2 \text{ s}^{-1}$, by some two orders of magnitude. We must conclude therefore, that exchange processes involving charged and neutral molecules will assist, or even dominate the electronic transport process perpendicular to the molecular columns.

Comparison of HAT5 and HAT6

In HAT5^{10,11} the results for hole transport in the mesophase appears to reflect a bandlike transport mechanism in one dimension. In contrast, in HAT6 the results reflect a more dispersive transport mechanism. This difference in the behavior of HAT6 and HAT5 is not easy to understand. It could be due to differences in sample preparation, thermal history, etc. Alternatively, dispersive transport is present in both HAT5 and HAT6, but the degree of dispersion is more marked in the latter. This is consistent with the relative mag-

nitudes of the hole mobilities measured in the two systems (HAT5 $\mu_{\parallel} \sim 1 \times 10^{-3} \text{ cm}^2 \text{ V}^{-1} \text{ s}^{-1}$ at 350 K, HAT6 $\mu_{\parallel} \sim 4.4 \times 10^{-4} \text{ cm}^2 \text{ V}^{-1} \text{ s}^{-1}$ at 350 K). We note that both of these values are too low to be consistent with ideal, bandlike transport.

Prospective applications

The hole mobility along the direction of the columns in the mesophase of HAT6, $\mu_{\parallel} \sim 1.0 \times 10^{-4} \text{ cm}^2 \text{ V}^{-1} \text{ s}^{-1}$, and the mechanism of charge transport along the columns, make HAT6 and conjugated discotic liquid crystals in general, a promising new class of high-resolution photoconductors. This is mainly due to the following:

(1) The absence of significant deep trapping in the current transients, a consequence of the liquidlike, self-healing²² properties of the molecular columns. Deep trapping and associated long-time tails is one of the main causes of undesirable memory effects in amorphous organic polymers commonly used in xerography and photolithography applications.³¹

(2) The relatively high mobility along the direction of the columns and the high anisotropy of the mobility. Hole mobilities along the direction of the columns are some two orders of magnitude greater than those typically observed in amorphous organic systems. The anisotropy of the mobility demonstrates that highly directional (quasi-one-dimensional) charge transport takes place, and that fabrication of high-resolution photoconductors is therefore a distinct possibility using discotic liquid crystals.

ACKNOWLEDGMENT

We wish to thank the EPSRC for financial support of this work.

¹S. Chandrasekhar and G. S. Raganath, Rep. Prog. Phys. **53**, 57 (1990).

²N. Boden, R. J. Bushby, J. Clements, M. V. Jesudason, P. F. Knowles, and G. Williams, Chem. Phys. Lett. **152**, 94 (1988); **154**, 613 (1989).

³N. Boden, R. J. Bushby, and J. Clements, J. Phys. Chem. **98**, 5920 (1993).

⁴L. Y. Chiang, J. P. Stokes, C. R. Safinya, and A. N. Bloch, Mol. Cryst. Liq. Cryst. **125**, 279 (1985).

⁵J. van Keulen, T. W. Warmerdam, R. J. M. Nolte, and W. Drenth, Recl. Trav. Chim. Pays Bas. **106**, 534 (1987).

⁶G. B. M. Vaughan, P. A. Heiney, J. P. McCauley, Jr., and A. B. Smith III, Phys. Rev. B **46**, 2787 (1992).

⁷N. Boden, R. J. Bushby, R. C. Borner, and J. Clements, J. Am. Chem. Soc. **116**, 10 807 (1994).

⁸N. Boden, R. J. Bushby, J. Clements, and R. Luo, J. Mater. Chem. (to be published).

⁹N. Boden, R. C. Borner, D. R. Brown, R. J. Bushby, and J. Clements, Liq. Cryst. **11**, 325 (1992).

¹⁰D. Adam, F. Closs, T. Frey, D. Funhoff, D. Haarer, H. Ringsdorf, P. Schuhmacher, and K. Siemensmeyer, Phys. Rev. Lett. **70**, 457 (1993).

¹¹D. Adam, D. Haarer, F. Closs, T. Frey, D. Funhoff, K. Siemens-

meyer, P. Schuhmacher, and H. Ringsdorf, Ber. Bunsenges. Phys. Chem. **97**, 1366 (1993).

¹²N. Boden, R. C. Borner, R. J. Bushby, A. N. Cammidge, and M. V. Jesudason, Liq. Cryst. **15**, 851 (1993).

¹³C. Destrade, M. C. Mondon, and J. Malthête, J. Phys. (Paris) Colloq. **40**, C3-18 (1979).

¹⁴D. Goldfarb, Z. Luz, and H. Zimmerman, J. Phys. (Paris) **42**, 1303 (1981).

¹⁵H. Scher and M. Lax, Phys. Rev. **7**, 4491 (1973); **7**, 4502 (1973).

¹⁶N. Karl, in *Defect Control in Semiconductors*, edited by K. Sumino (Elsevier Science, North-Holland, Amsterdam, 1990).

¹⁷H. Bottger and V. V. Bryskin, *Hopping Conduction in Solids* (VCH, Berlin, 1985).

¹⁸S. Alexander, J. Bernasconi, W. R. Schneider, and R. Orbach, Rev. Mod. Phys. **53**, 175 (1981).

¹⁹D. Adam, P. Schumacher, J. Simmerer, L. Hausling, K. Siemensmeyer, K. H. Eitzbach, H. Ringsdorf, and D. Haarer, Nature (London) **371**, 141 (1994).

²⁰P. Sheng, Phys. Rev. B **21**, 2180 (1980).

²¹B. Movaghar, in *Proceedings of The 5th International Autumn School*, Warsaw, Poland, edited by J. Przyluski and S. Roth (Trans. Tech, Switzerland, 1995).

- ²²I. G. Voigt-Martin, R. W. Garbella, and M. Schumacher, *Liq. Cryst.* **17**, 775 (1994).
- ²³R. Y. Dong, D. Goldfarb, M. E. Moseley, Z. Luz, and H. Zimmerman, *J. Phys. Chem.* **88**, 3148 (1984).
- ²⁴P. M. Borsenberger, L. Pantmeier, and H. Bässler, *J. Chem. Phys.* **94**, 5447 (1991).
- ²⁵P. G. Schouten, J. M. Warman, M. P. deHaas, J. F. Van der Pol, and J. W. Zwicker, *J. Am. Chem. Soc.* **114**, 9028 (1992); P. G. Schouten, J. M. Warman, M. P. deHaas, C. F. Vannostrum, G. H. Gelinck, R. J. M. Nolte, M. J. Copyn, J. W. Zwicker, M. K. Engel, M. Hanack, Y. H. Cang, and W. T. Ford, *ibid.* **116**, 6880 (1994).
- ²⁶B. Movaghar, B. Pohlmann, and D. Würtz, *Z. Phys. B* **66**, 523 (1987).
- ²⁷H. Aoyama and T. Odagaki, *J. Phys. A* **20**, 4985 (1987).
- ²⁸R. Bruinsma and P. Bak, *Phys. Rev. Lett.* **56**, 420 (1986).
- ²⁹A. Yelon, B. Movaghar, and H. Branz, *Phys. Rev. B* **46**, 244 (1992).
- ³⁰R. A. Marcus, *Ann. Rev. Phys. Chem.* **16**, 155 (1964); J. Ulstrup, *Charge Transfer Processes in Condensed Media* (Springer, New York, 1979).
- ³¹P. M. Borsenberger and D. S. Weiss, in *Handbook of Imaging Materials*, edited by A. S. Diamond (Marcel Dekker, New York, 1991).